Available online at www.sciencedirect.com
ScienceDirect
Journal of Sound and Vibration 324 (2009) 317–331
JOURNAL OF SOUND AND VIBRATION
www.elsevier.com/locate/jsvi

The antioscillator model and the finite element method

E. Jacquelin[a,*], J.-P. Lainé[b], M. Massenzio[a]

[a]*Université de Lyon, Université Claude Bernard Lyon I, INRETS, UMR-T 9406, LBMC, IUT B, 17 rue de France, 69627 Villeurbanne, France*
[b]*Ecole Centrale de Lyon, LTDS, 36 Av. Guy de Collongue, 69134 Ecully, France*

Received 1 April 2008; received in revised form 15 January 2009; accepted 19 January 2009
Handling Editor: M.P. Cartmell
Available online 25 February 2009

Abstract

A finite element model of a structure can provide useful knowledge of the structural response but such a model may also lead to a misunderstanding of the structure's behaviour. That is why a new model was developed, namely the antioscillator model. This paper explains how the antioscillator model can be obtained from a finite element model. The antioscillator model is particularly suitable for dealing with impact problems; for instance, it can provide parameters that have physical meaning, and can be used to forecast several impact results (the duration of impact for example). Moreover, it is shown how this model may select optimal degrees-of-freedom for simulations such that some dof can then be disregarded and the others are assumed to be necessary and sufficient.

1. Introduction

The most commonly used technique for structural modelling is the finite element (FE) method [1]. This is well-adapted for solving dynamic problems, such as cases of impact between structures. The drawback can be for misunderstanding of the global phenomena involved. This may lead to a non-efficient model perhaps with too many degrees-of-freedom (dof) when in fact a few dof may be sufficient.

This scenario is often the case for low velocity impacts, as considered in this paper. Indeed, very simple models have been used efficiently to determine the impact force. A single dof system connected to the impactor (a rigid mass) through a nonlinear interaction spring has been shown to be suitable and sufficient for evaluating the structural response [2–4]. The stiffness of that single dof system can be determined by the static stiffness combined with some other structural aspects [2] such as membrane stiffness, shear stiffness, etc. Likewise, the interaction spring stiffness k_{contact} can be derived from a contact law that can be determined experimentally [5]. The Hertz contact law will be considered in this paper.

Nevertheless, these models allow for the first eigenmode of the structure only. Jacquelin et al. [6,7] have extended this model now called the antioscillator (AO) model and, have shown how to derive its parameters

*Corresponding author. Tel.: +33 472 692132; fax: +33 472 692120.
E-mail address: eric.jacquelin@univ-lyon1.fr (E. Jacquelin).

0022-460X/$ - see front matter © 2009 Elsevier Ltd. All rights reserved.
doi:10.1016/j.jsv.2009.01.041

experimentally. In this paper it will be shown how to get such a model from the structural FE model, and that such a model will significantly reduce the number of dof.

The AO description is linked to a given dof i_0 i.e., to a point on the studied structure and to a direction. The use of the direction of an action effect, an impact force direction for instance, can lead to a very efficient model. That is why this description suits to impact problems very well particularly when the impact location and direction are known. Also this approach is general and may be used with all kind of loads and, above all, it can explain how the global structure behaves when excited in specific dof i_0 [8].

This paper may be viewed as a companion paper to the article by Jacquelin et al. [6] in which a very general presentation may be found. First a practical presentation of AO model based on a FE model is given in the present paper. Then a dof selection criterion is proposed in order to be able to disregard some of the dof. Likewise, a truncation of the response expansion is presented to reduce the dof number. Finally, some examples are given to show the efficiency and simplicity of the method, and to evaluate the selection and truncation criteria.

2. The AO model

A dynamic test is considered in which the driven point and the measurement point are collocated. The frequency response function presents some maxima (associated with the resonance frequencies) and some minima (associated with the antiresonant frequencies). The maxima depend only on the structure characteristics whereas the minima depend on the structure characteristics and on the measurement/driven point as well. The AO model is linked to the antiresonant frequencies, as indicated in the following. Therefore for each point on a structure it is possible to establish an AO model. More precisely, the AO model depends on a dof associated with the point of interest. In the following, the dof associated with a AO model is referred to as "i_0".

The mass ($\mathbf{M}^{\mathrm{FE}}$) and stiffness ($\mathbf{K}^{\mathrm{FE}}$) matrices of the FE model are supposed to be known *a priori*; n is the model dof number, $\mathbf{X}(t)$ is the dof vector and $\mathbf{F}(t)$ is the load vector.

2.1. Static, constraint and residual modes

Traditionally, problems in structural dynamics require a discretisation technique to be implemented. The FE method is probably the most popular discretisation method. The AO method is based on some specific Rayleigh–Ritz vectors which may be easily derived from a first FE model. To define these vectors requires some specific matrices and vectors associated with the chosen dof i_0:

- the AO mass $\mathbf{M}^{\mathrm{AO}}$ (AO stiffness $\mathbf{K}^{\mathrm{AO}}$) matrix: This matrix is derived from the FE mass (stiffness) matrix by replacing the i_0th row and the i_0th column by a row and a column filled with zeros;
- the static load $\mathbf{F}_{\mathrm{st}}$: This is an n-size vector such as all of its elements are zero except the i_0th element; the ith element is

$$\mathbf{F}_{\mathrm{st}\,i} = \mathbf{F}_{\mathrm{st}\,i}\delta_{i\,i_0} \tag{1}$$

where δ is the Kronecker symbol.

The static load vector has no link with the actual loads applied to the structure. Indeed this vector is introduced as a way to account for the i_0 dof.

The following modes can then be defined:

- The constraint modes $\{\boldsymbol{\phi}_i, \omega_{\mathrm{AR}\,i}\}_{i=1\ldots n-1}$ are the solution of the eigenproblem associated with the AO mass matrix and the AO stiffness matrix; hence the eigenvectors $\{\boldsymbol{\phi}_i\}_{i=1\ldots n-1}$ cancel out for the i_0 dof,

$$\boldsymbol{\phi}_{i\,i_0} = 0 \tag{2}$$

Accordingly, the associated eigenfrequencies belong to the set of the antiresonant frequencies [9].

- The static mode $\boldsymbol{\phi}_{\mathrm{st}}$ is a dof vector such that,

$$\mathbf{K}^{\mathrm{FE}}\boldsymbol{\phi}_{\mathrm{st}} = c_{\mathrm{st}}\mathbf{F}_{\mathrm{st}} \tag{3}$$

$$\boldsymbol{\phi}_{\mathrm{st}\,i_0} = 1 \tag{4}$$

where we have to distinguish the statically determinate and indeterminate structures to define c_{st}:

  - statically determinate structures $c_{\mathrm{st}} = 1$,

$$\boldsymbol{\phi}_{\mathrm{st}} = (\mathbf{K}^{\mathrm{FE}})^{-1}\mathbf{F}_{\mathrm{st}} \tag{5}$$

  - statically indeterminate structures $c_{\mathrm{st}} = 0$ and $\boldsymbol{\phi}_{\mathrm{st}}$ is a rigid body mode.

- The residual mode $\boldsymbol{\phi}_0$ is a vector which verifies,

$$\boldsymbol{\phi}_0 = \boldsymbol{\phi}_{\mathrm{st}} - \sum_{i=1}^{n-1} c_i\boldsymbol{\phi}_i \tag{6}$$

$$\forall i \geqslant 1, \quad \boldsymbol{\phi}_0^t\mathbf{M}^{\mathrm{FE}}\boldsymbol{\phi}_i = 0 \tag{7}$$

The orthogonality property (7) leads to

$$c_i = \frac{\boldsymbol{\phi}_i^t\mathbf{M}^{\mathrm{FE}}\boldsymbol{\phi}_{\mathrm{st}}}{\boldsymbol{\phi}_i^t\mathbf{M}^{\mathrm{FE}}\boldsymbol{\phi}_i} \tag{8}$$

Then, the dof vector $\mathbf{X}$ may be expanded in terms of a sum of the Rayleigh–Ritz vectors $\{\boldsymbol{\phi}_i\}_{i=1\cdots n-1}$:

$$\mathbf{X}(t) = \sum_{i=0}^{n-1} q_i(t)\boldsymbol{\phi}_i \tag{9}$$

2.2. Antioscillators

The dof vector expansion (9) may be reorganised as follows:

$$\begin{aligned}\mathbf{X}(t) &= q_0(t)\left(\boldsymbol{\phi}_{\mathrm{st}} - \sum_{i=1}^{n-1} c_i\boldsymbol{\phi}_i\right) + \sum_{i=1}^{n-1} q_i(t)\boldsymbol{\phi}_i \\ &= q_0(t)\boldsymbol{\phi}_{\mathrm{st}} + \sum_{i=1}^{n-1}\left(\frac{q_i(t)}{c_i} - q_0(t)\boldsymbol{\phi}_i\right)c_i\boldsymbol{\phi}_i \\ &= \lambda_0(t)\boldsymbol{\psi}_0 + \sum_{i=1}^{n-1}(\lambda_i(t) - \lambda_0(t))\boldsymbol{\psi}_i\end{aligned} \tag{10}$$

where

$$\lambda_0(t) = q_0(t) = \mathbf{X}_{i_0}, \quad \boldsymbol{\psi}_0 = \boldsymbol{\phi}_{\mathrm{st}}$$

$$\lambda_i(t) = \frac{q_i(t)}{c_i}, \quad \boldsymbol{\psi}_i = c_i\boldsymbol{\phi}_i$$

The parameter λ_0 is the i_0 dof, $\mathbf{X}_{i_0}$.

This change of variables leads to the striking model depicted in Fig. 1 where the dof are the parameters $\{\lambda_i\}_{i=0\ldots n-1}$ and the first single dof system (m_0, k_0) is the basis of the $n-1$ single dof systems $(m_i, k_i)_{i=1\ldots n-1}$, which are called the AOs. The AO parameters $(m_i, k_i)_{i=0\ldots n-1}$ must be defined as well as the load vector $\mathbf{F}^{\mathrm{AO}}$.

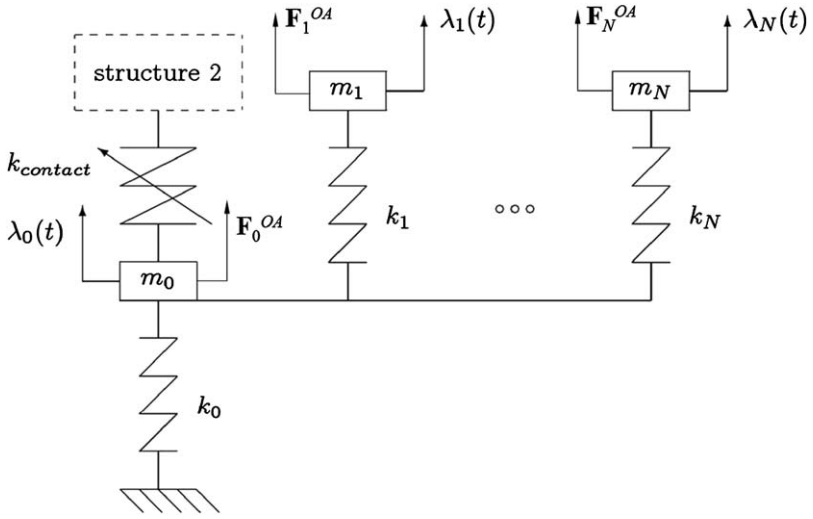

Fig. 1. AO model of any structure.

2.2.1. Masses $\{m_i\}_{i=0\ldots n-1}$

The kinetic energy of the structure is derived in term of parameters λ_i. By comparing it to the kinetic energy of the system represented in Fig. 1, it may be proved (see Appendix A) that

$$\forall i \geqslant 1, \quad m_i = c_i^2 \boldsymbol{\phi}_i^t \mathbf{M}^{\mathrm{FE}} \boldsymbol{\phi}_i = \frac{(\boldsymbol{\phi}_i^t \mathbf{M}^{\mathrm{FE}} \boldsymbol{\phi}_{\mathrm{st}})^2}{\boldsymbol{\phi}_i^t \mathbf{M}^{\mathrm{FE}} \boldsymbol{\phi}_i} \tag{11}$$

$$m_0 = \boldsymbol{\phi}_{\mathrm{st}}^t \mathbf{M}^{\mathrm{FE}} \boldsymbol{\phi}_{\mathrm{st}} - \sum_{i=1}^{n-1} m_i = m_{\mathrm{st}} - \sum_{i=1}^{n-1} m_i \tag{12}$$

Expression (12) suggests that m_0, as the difference between a "static" mass m_{st} (the one involved in the static mode) and the masses $\{m_i\}_{i=1\ldots n-1}$, may be viewed as the residual mass. Relation (11) shows that the masses are independent of the norm of the eigenshapes $\{\boldsymbol{\phi}_i\}_{i=1\ldots n-1}$.

2.2.2. Stiffnesses $\{k_i\}_{i=0\ldots n-1}$

Similarly, in Appendix B it has been proved that the deformation energy of the structure may be identified to the deformation energy of the AO-model:

- $$k_0 = \boldsymbol{\phi}_{\mathrm{st}}^t \mathbf{K}^{\mathrm{FE}} \boldsymbol{\phi}_{\mathrm{st}} \tag{13}$$
  - For statically determinate structures, k_0 is the static stiffness.
  - For statically indeterminate structures (i.e., $\boldsymbol{\phi}_{\mathrm{st}}$ is a rigid body eigenvector), $k_0 = 0$.
- $$\forall i \geqslant 1, \quad k_i = \omega_{\mathrm{AR}\,i}^2 m_i \tag{14}$$

2.2.3. Force vector

By considering the balance equation of the structure, it has been proved in Appendix C that,

$$\mathbf{F}_0^{\mathrm{AO}} = \boldsymbol{\phi}_0^t \mathbf{F} \tag{15}$$

$$\forall i \geqslant 1, \quad \mathbf{F}_i^{\mathrm{AO}} = c_i \boldsymbol{\phi}_i^t \mathbf{F} \tag{16}$$

3. A reduced AO model

In the following the AOs have been sorted according to their ascending natural frequencies.

An AO model will be more interesting than a FE model from a simulation point of view if it is possible to provide a model order reduction. That is possible by implementing the following:

- disregarding *a priori* some AOs,
- truncating the following expansion:

$$X(t) = \lambda_0(t)\psi_0 + \sum_{i=1}^{n-1}(\lambda_i(t) - \lambda_0(t))\psi_i$$

3.1. AO selection

We next consider a symmetric structure with a load applied along the axis of symmetry. It is well known that the eigenmodes are either symmetric or antisymmetric, the higher modes are not excited and that the generalised coordinates associated with these modes cancel out. Nevertheless, a mode expansion does not give a criterion for determining that such a generalised coordinate can be disregarded. The antisymmetric modes are in the constraint mode set as well, and they do not take part in the response. Hence they must not be considered. It turns out that the AO masses associated with these constraint modes then cancel out. More generally, when an eigenmode corresponds to a constraint mode i, the AO mass m_i is equal to zero. The proof is given in Appendix D. So a criterion is highlighted for disregarding an AO, and therefore if an AO has a mass equal to zero then that AO is disregarded.

Obviously, from a numerical point of view a zero-mass means a mass below a given threshold mass. More precisely, in the following, the threshold mass will be scaled by the maximum AO mass because an absolute threshold is impossible to define.

3.2. Truncation

Fig. 1 suggests that the AO displacement may be closed to the residual mass displacement when the AO number is high enough, noting that there is some subjectivity associated with this decision. Indeed, if the AO number i is high enough, the frequency $\omega_{\mathrm{AR}\,i}$ may be very large, and that would make $\lambda_i(t)$ almost equal to $\lambda_0(t)$. All the AOs which have the same displacement as the residual mass behave as the residual mass. In other words it is not necessary to consider their displacements as additional dof; rather the masses related to these AOs must be gathered in to the residual mass. Then, such a truncation does not introduce any unrealistic lack of mass.

To evaluate if an AO displacement is close to the residual mass displacement, the discrepancy $\mathscr{D}_i$ between the ith AO and the residual mass can be introduced, as follows:

$$\mathscr{D}_i = \frac{\|\lambda_i - \lambda_0\|_2}{\|\lambda_0\|_2} \tag{17}$$

Then a truncated model may be obtained by defining a discrepancy threshold. All the AO with a discrepancy lower than the threshold should be truncated.

Obviously, this approach does not show how the discrepancy threshold should be determined. Nevertheless, it seems that we can have some *a priori* information about the discrepancy by correlating the discrepancy and the AO mass distribution. This will be examined in the following examples.

4. A first example: the axial impact of two free–free bars

The axial impact of two identical free–free bars has been considered as a way of addressing the truncation issue. The bars are made up of steel with circular cross section and hemispherical ends at the point of impact. The material and geometrical properties of the bars are given in Table 1.

The Hertz contact stiffness has been evaluated to be $k_H = 2.9 \times 10^{10}\,\mathrm{N\,m^{-3/2}}$, for an end curvature of 70 mm. The initial relative velocity is $0.4\,\mathrm{m\,s^{-1}}$.

A numerical integration of the equations has been performed with an implicit β–γ Newmark method coupled with a Newton–Raphson technique to account for the nonlinear interaction force:

$$\mathbf{F}_{\mathrm{nl}} = k_H(\mathbf{X}^2_{i_0} - \mathbf{X}^1_{i_0})^{3/2} \tag{18}$$

where $\mathbf{X}^i$ is the FE model dof vector associated with the bar i; $\mathbf{X}^i_{i_0}$ is the dof associated with the bar i AO model, $\mathbf{F}_{nl}$ is the Hertz interaction force vector (due to bar 2 on bar 1).

4.1. The FE modelling

Each bar has been discretised in n_e two-node elements, with 1 dof per node and a linear interpolation for the displacement. Hence a mass matrix $\mathbf{M}^{\mathrm{FE}}_i$ and a stiffness matrix $\mathbf{K}^{\mathrm{FE}}_i$ has been built for each bar i from the FE model. A direct integration provided the reference solution.

4.2. The modal model

The solution of this structural problem has been obtained from the dof vector mode expansion as well. The eigenvectors have been calculated by solving the eigenproblem associated with the mass and stiffness matrices $\mathbf{M}^{\mathrm{FE}}_i$ and $\mathbf{K}^{\mathrm{FE}}_i$ for each impacting structure i. The interaction force is calculated at each computation step by combining the modal variables to evaluate the displacement for each structure at the impact point. This method is very useful if a truncation of the mode expansion is implemented in order to reduce the number of dof involved in the FE modelling.

4.3. The AO model

The mass and stiffness matrices $\mathbf{M}^{\mathrm{AO}}_i$ and $\mathbf{K}^{\mathrm{AO}}_i$ have been obtained from the $\mathbf{M}^{\mathrm{FE}}_i$ and $\mathbf{K}^{\mathrm{FE}}_i$ for the dof i_0. The eigenmodes of the $\mathbf{M}^{\mathrm{AO}}_i$ and $\mathbf{K}^{\mathrm{AO}}_i$ matrices are the constraint modes of the structure i; the "static" mode is a rigid body mode that was easily obtained from $\mathbf{M}^{\mathrm{FE}}_i$ and $\mathbf{K}^{\mathrm{FE}}_i$. The characteristics of the first AOs are listed in Table 2. The "static" mass is actually the bar mass $m_{\mathrm{st}} = 1.73\,\mathrm{kg}$ and the stiffness k_0 is equal to zero, for a statically indeterminate structure.

Interestingly, the interaction force is directly computed because $\lambda^i_{i_0} = \mathbf{X}_{i\,i_0}$ ($i = 1$ or 2), as follows:

$$\mathbf{F}_{\mathrm{nl}} = k_H(\lambda^2_{i_0} - \lambda^1_{i_0})^{3/2} \tag{19}$$

Table 1
Properties of the impacting bar i ($i = 1, 2$).

E (GPa)	ρ ($\mathrm{kg\,m^{-3}}$)	d (mm)	L (mm)
210	7800	30	313

Table 2
Characteristics of the AO bar model.

AO number	1	2	3	4
Mass (kg)	1.40	0.16	0.06	0.03
Stiffness ($10^8\,\mathrm{N\,m^{-1}}$)	9.49	9.48	9.51	9.52

4.4. Simulations for an axial impact of two free–free bars

The modelling with the eigenmodes or the AOs offers a possibility for truncating an expansion. So the next simulations will permit a comparison of the results. The interaction force and the stresses in one bar are presented.

The bars have been discretised into 49 elements. Hence, the FE model has 50 dof. Some simulations have been carried out for the full FE model, the AO model, and the modal model.

The interaction forces given by the FE model, the 3-dof modal model and the 3-dof AO model, are in very good agreement (see Fig. 2). More precisely, the FE results and the 3-dof AO model give an almost perfect overlay.

Fig. 3a compares the stresses obtained from the 3-dof AO model and the FE model, whereas Fig. 3b compares the stresses obtained from the 3-dof modal model and the FE model. It is shown that 3 dof are enough for the AO model for obtaining results as good as those of the FE model, whereas the modal model gives much less accurate results for the same dof number.

Moreover, the locations for the measurements are seen to be far from the impacted end of the bar. Hence the stress wave has had to travel, and no signal has been able to be recorded before 5 μs at the first point and 19 μs at the second point. Fig. 4 shows that no perturbation has occurred before these durations when the AO model is used, even with few dof. Accordingly, the AO model allows for wave propagation although, that is not obvious from the AO-model scheme depicted in Fig. 1.

4.5. Truncation criterion

The curves plotted in Figs. 3 and 4 show the sensitivity to the truncation order. Fig. 5 shows that the AO displacement is close to the residual mass displacement when the AO number is greater or equal to two. The discrepancies of the AO have been evaluated: $\mathscr{D}_i$ is lower than 0.4%, except for the first AO ($\mathscr{D}_1 \simeq 2.8\%$). Then, all the AOs except the first one behave almost as the residual mass. Hence a truncated model could be obtained by defining a discrepancy threshold. It is set to 1% for maximum discrepancy so the ratio of an AO discrepancy to the maximum discrepancy has had to be evaluated. As suggested in the previous section, the ratio of the AO masses to the greatest AO mass are compared to the ratio of the discrepancies to the greatest discrepancy. Fig. 6 shows that both are very similar. Therefore the 1% threshold has been applied to the AO mass ratio. Five AOs are then considered (see Fig. 6) and the others are gathered in to the residual mass. The interaction force and the stresses can be evaluated with five AOs, and the results give almost the same curves as those plotted in Figs. 2a and 4. This then validates the 1% threshold for this example.

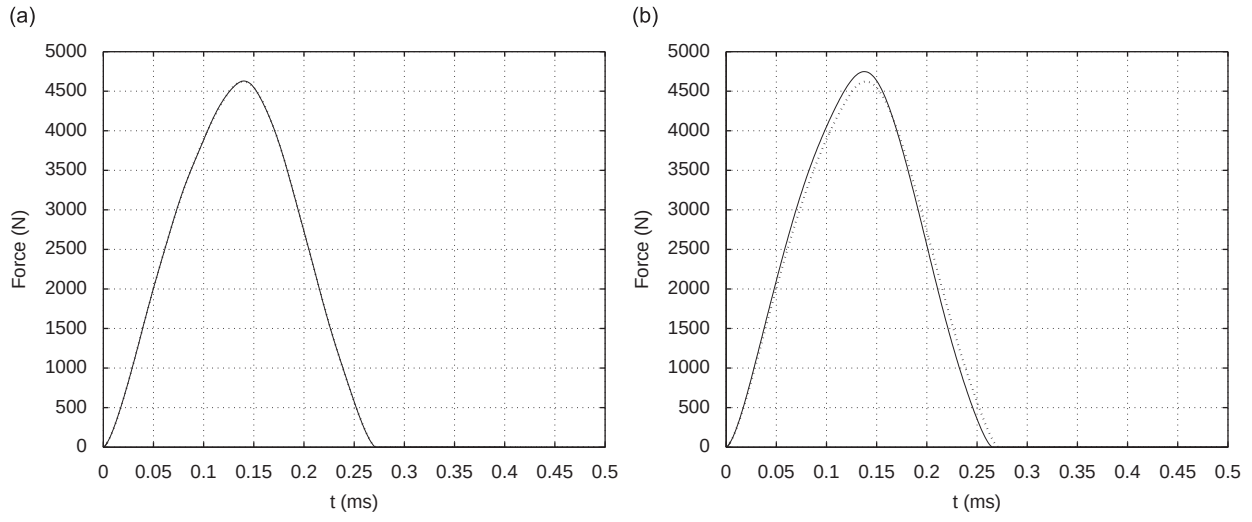

Fig. 2. Interaction force: FE model: 50 dof (...); (a) antioscillators model: 3 dof (–); (b) modal model: 3 dof (–).

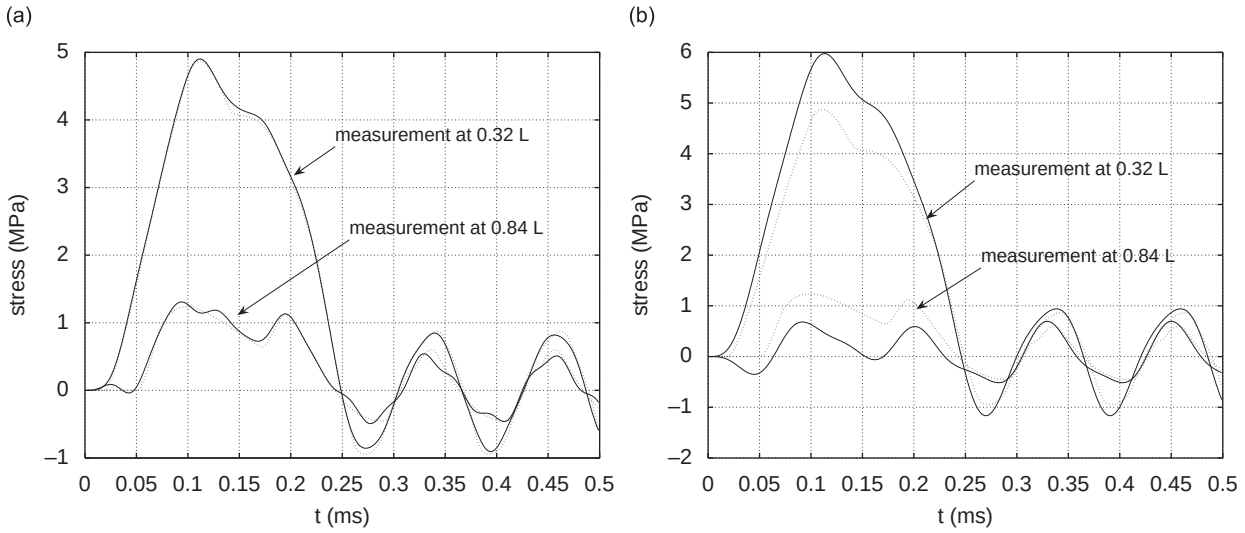

Fig. 3. Stress at the positions $x = 0.32 \times L$ and $0.84 \times L$: FE model: 50 dof (...); (a) antioscillators model: 3 dof (–); (b) modal model: 3 dof (–).

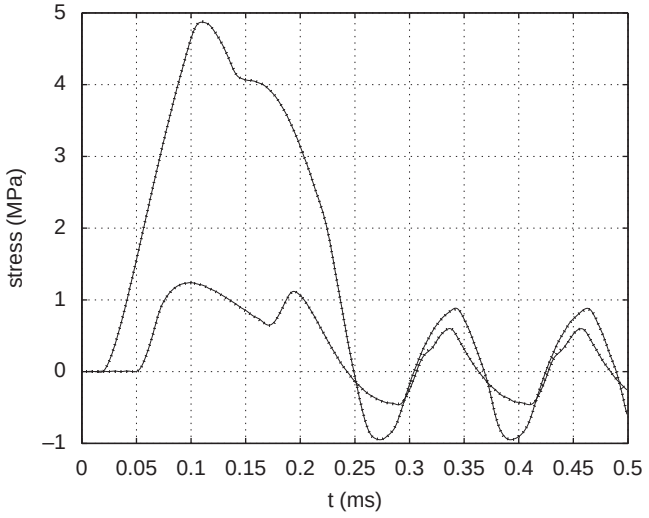

Fig. 4. Stress at the positions $x = 0.32 \times L$ and $0.84 \times L$: FE model: 50 dof (...); antioscillators model: 10 dof (–).

5. Second example: a solid impacted by a rigid mass

This example aims to prove that the AO-model may be built easily even for more complex structures, 3D solids for instance. Once again, the efficiency of the method for simulating an impact event is presented.

5.1. Description of the structure

A simply supported beam is considered in this section: a 3D FE is used to model this solid. The element is defined by eight nodes having 3 dof (translations) at each node and by a linear interpolation with respect to each direction. The element number in the x, y and z direction is, respectively, 50, 2 and 2.

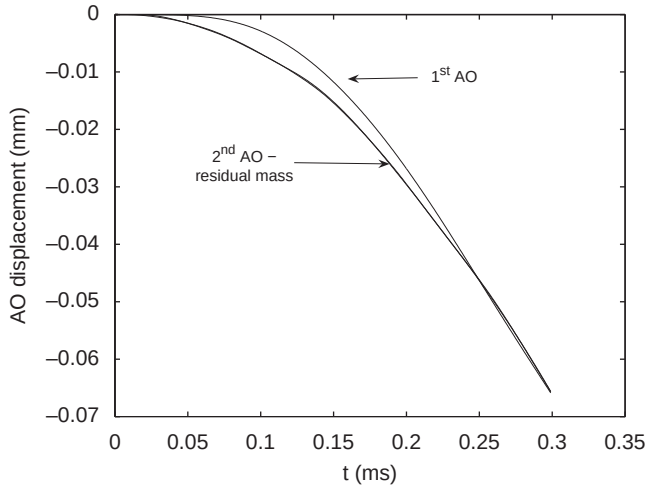

Fig. 5. Displacement of the first two AO—displacement of the residual mass.

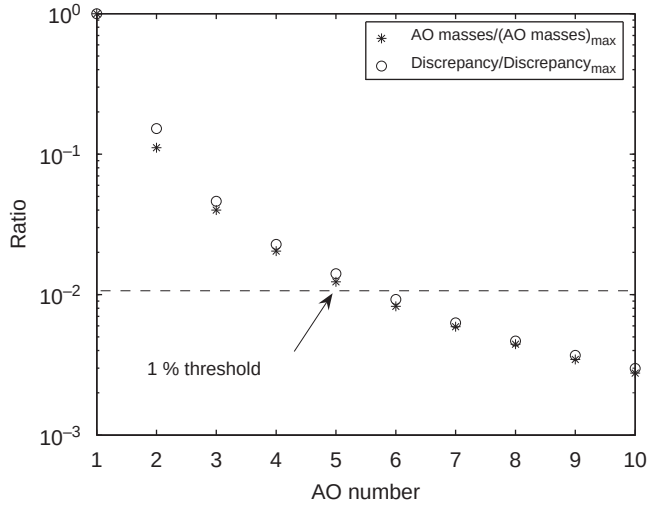

Fig. 6. Ratio of the AO masses to the greatest AO mass—discrepancy ratio.

Table 3
Properties of the solid.

E (GPa)	ρ (kg m^{-3})	a (mm)	L (m)
70	2400	20	1

The beam has a square section ($a \times a$), Young's modulus E, density ρ and length L. The beam characteristics are listed in Table 3.

The boundary conditions have been set as follows:

- the left lower end ($x = 0$, $z = 0$) is grounded to the x-axis, y-axis and z-axis;
- the right lower end ($x = L$, $z = 0$) is grounded to the y-axis and z-axis.

The full FE model has 1362 dof.

5.2. The truncation criterion

The beam is impacted by a spherical mass (radius R) at the centre of the top surface. The impact velocity v_{impact} is parallel to the z-axis. As the impact force location and direction are known, we are able to derive the AO model from the mass and stiffness matrices according to Section 2. The characteristics of the first 6 AOs are listed in Table 4.

The Hertz law is used to describe the contact conditions between both solids and the Hertz stiffness k_H is given in Table 5. The spherical mass is considered as a rigid solid, see the properties in Table 5.

The mid-span displacement of the beam and the displacement of the mass are both shown in Fig. 7; the impact force is illustrated in Fig. 8. Two models have been used to obtain these results. One is based on the AOs and the other one is from a mode superposition analysis. Both of them are derived from the FE model and give the same results, but they do not have the same dof number: 11 AOs, i.e. 12 dof, are enough to obtain the results, whereas 40 modes are required.

In fact this example illustrates very well the AO selection discussed in Section 3. Indeed, considering the first eigenmode the shape is seen to be in the xy-plane. Therefore this mode does not have any actual influence on the response because the impact velocity is parallel to the z-axis. The generalised coordinate associated with the first mode should be disregarded and this is the same for all the modes with eigenshapes in the xy-plane. It is not easy to detect such features for the eigenshapes; thus no generalised coordinates are disregarded. On the

Table 4
Characteristics of the AO beam model.

AO number	1	2	3	4	5	6
Mass (g)	0.038	248.6	1.5	55.2	22.4	0.2
Stiffness ($10^6\,\text{N m}^{-1}$)	80×10^{-6}	1.28	0.05	2.70	1.61	0.03

Table 5
Properties of the sphere.

Mass	R (mm)	k_H ($\text{N m}^{-3/2}$)	v_{impact} (m s^{-1})
$\frac{m_{\text{beam}}}{2}$	10	7.8×10^9	0.01

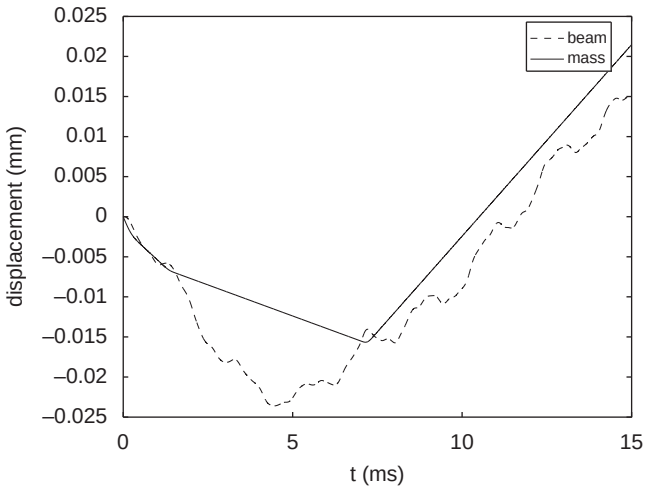

Fig. 7. Mid-span displacement of the beam—displacement of the mass.

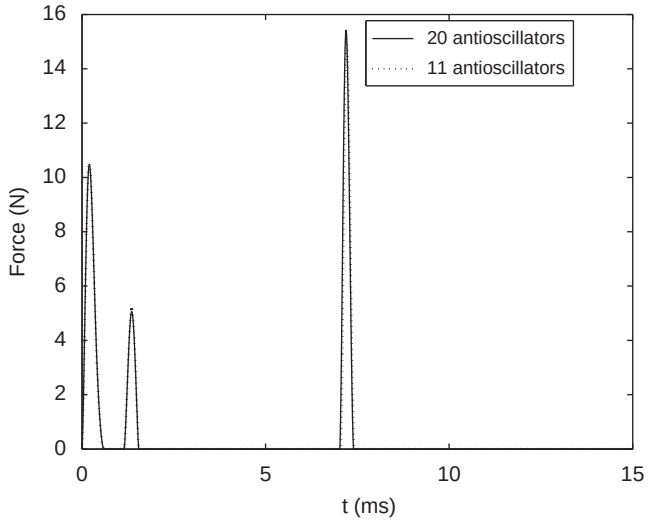

Fig. 8. Interaction force.

Fig. 9. Third mode eigenshape.

contrary, the AO-model may easily detect whether a constraint mode has negligible influence by evaluating the mass of the corresponding AO, as indicated in Section 3. In the simulations all the AOs that have a mass less than $10^{-5} \times m_{st}$ can be neglected. It is found that a constraint mode with a shape that exists in the xy-plane provides a mass which is almost-zero i.e. lower than $10^{-20} \times m_{st}$. Then, such a constraint mode does not provide an AO.

Likewise a constraint mode corresponding to an eigenmode has a zero mass as well, see Appendix D. That is the case when the dof i_0 is also a modal node. In the studied case the structure is not exactly symmetric with respect to the mid-span section, due to the nonsymmetric boundary conditions. Nevertheless Fig. 9 shows that the third eigenshape is almost antisymmetric with respect to the mid-span section; accordingly this mode corresponds almost exactly to the second constraint mode and that was also proved by comparing the frequencies. The eigenfrequency is 232.55 Hz and the antiresonant frequency is 232.57 Hz. Then we find that the ratio of the corresponding mass to the static mass is 8×10^{-5}. This AO is not disregarded because the criterion has been to neglect the AOs that have a mass less than $10^{-5} \times m_{st}$ but in fact its influence on the response is negligible. In the studied case, only 20 AOs have a mass greater than $10^{-5} \times m_{st}$. But the 1st, 3rd, 6th, 8th, 11th and 18th AOs, see Fig. 10, have a negligible influence on the response. All those AOs correspond to a constraint mode which is also an (almost) eigenmode of the structure. That is proved in Fig. 8 where the impact forces obtained with 11 AOS and 20 AOs are seen to be the same.

Thus, if the threshold is $10^{-4} \times m_{st}$, then these AO would have been automatically disregarded and then 11 AOs would have be found immediately.

Moreover, a truncation had been done according to Section 3. The discrepancy threshold has been set to 1% of the maximum discrepancy. As observed in Fig. 6, Fig. 10 shows that the discrepancy ratio trend was very similar to the AO mass ratio trend. So the 1% threshold is set on the mass ratio: 11 AOs are finally considered. The impact force obtained with 11 AOs and 20 AOs is in an excellent agreement, Fig. 8. This example validates the 1% threshold.

Thus, when a truncation is achieved, the first n constraint modes that provide a mass greater than a given threshold are considered. Accordingly, the parameters used to describe the response are in a certain way optimised and lead to less dof than the mode expansion analysis.

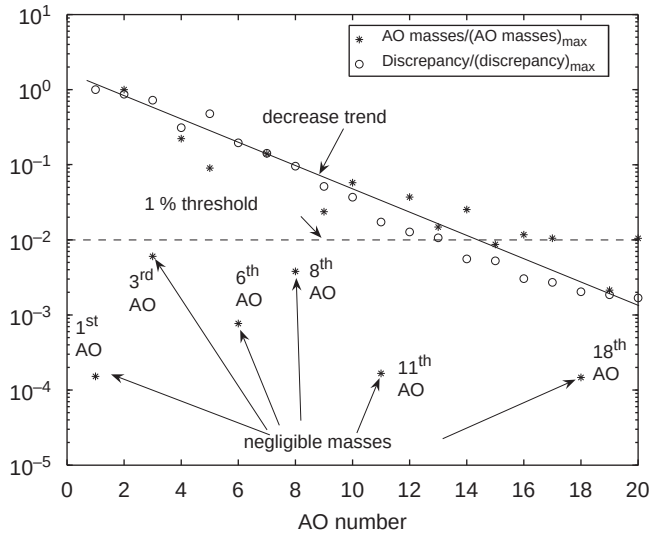

Fig. 10. Ratio of the AO masses to the greatest AO mass—discrepancy ratio.

6. Conclusions

It has been shown that any FE model may be transformed into an equivalent spring-mass set system in a form of an AO model. From a simulation point of view, this is very useful for the explicit integration methods because the AO model leads directly to a diagonal mass matrix.

The different examples have shown that the AO model makes it possible to select the AOs because it is easy to forecast their influence on the response. That leads to a decrease in the number of dof when this approach is used. The criterion used to disregard an AO is based on the discrepancies between the response of the AOs and the residual mass. Both examples show a striking similarity between these discrepancies and the AO mass distribution. This provides a criterion for selecting the significant AOs. Indeed, the first example shows that the first AO has a major role in the impact problem. In the first example the first AO mass represents more than 80% of the bar mass. That explains why only two AOs are enough to simulate correctly the impact force. In the second example the first AO mass is more than 50% of the static mass. It is a large proportion of the mass, but it is not enough to simulate accurately the structural response. That is why more AOs are required.

Obviously this AO model has a cost due to the constraint mode computation. Moreover, if the force location changes, those antimodes will have to be computed as well. But we must keep in mind that the first interest of the AO model is to understand the structure behaviour better as shown by Pashah et al. [8]. Sometimes a better comprehension of the structure behaviour may avoid some unnecessary calculations.

Appendix A. Masses $\{m_i\}_{i=0\ldots n-1}$

The masses may be deduced from the kinetic energy $\mathscr{T}$:

$$\mathscr{T} = \tfrac{1}{2}\dot{\mathbf{X}}^t \mathbf{M}^{\mathrm{FE}} \dot{\mathbf{X}} \tag{A.1}$$

The dof vector expression (9) and the eigenvector orthogonality properties lead to the following kinetic energy expression:

$$\mathscr{T} = \frac{1}{2}\sum_{i=0}^{n-1} \dot{q}_i^2 \boldsymbol{\phi}_i^t \mathbf{M}^{\mathrm{FE}} \boldsymbol{\phi}_i = \frac{1}{2}\dot{\lambda}_0^2 \boldsymbol{\phi}_0^t \mathbf{M}^{\mathrm{FE}} \boldsymbol{\phi}_0 + \frac{1}{2}\sum_{i=1}^{n-1} c_i^2 \dot{\lambda}_i^2 \boldsymbol{\phi}_i^t \mathbf{M}^{\mathrm{FE}} \boldsymbol{\phi}_i \tag{A.2}$$

So the masses depicted in Fig. 1 are defined by

- $i>0$:

$$m_i = c_i^2 \boldsymbol{\phi}_i^t \mathbf{M}^{\mathrm{FE}} \boldsymbol{\phi}_i = \frac{(\boldsymbol{\phi}_i^t \mathbf{M}^{\mathrm{FE}} \boldsymbol{\phi}_{\mathrm{st}})^2}{\boldsymbol{\phi}_i^t \mathbf{M}^{\mathrm{FE}} \boldsymbol{\phi}_i} \tag{A.3}$$

- $i=0$:

$$m_0 = \boldsymbol{\phi}_0^t \mathbf{M}^{\mathrm{FE}} \boldsymbol{\phi}_0 \tag{A.4}$$

The definition of $\boldsymbol{\phi}_0$ given by (6), the eigenvector orthogonality property and the definition of the coefficient c_i, (8), lead to the following result:

$$\begin{aligned} m_0 &= \boldsymbol{\phi}_0^t \mathbf{M}^{\mathrm{FE}} \boldsymbol{\phi}_0 = \boldsymbol{\phi}_{\mathrm{st}}^t \mathbf{M}^{\mathrm{FE}} \boldsymbol{\phi}_{\mathrm{st}} - 2\sum_{i=1}^{n-1} c_i \boldsymbol{\phi}_i^t \mathbf{M}^{\mathrm{FE}} \boldsymbol{\phi}_{\mathrm{st}} + \sum_{i=1}^{n-1} c_i^2 \boldsymbol{\phi}_i^t \mathbf{M}^{\mathrm{FE}} \boldsymbol{\phi}_i \\ &= \boldsymbol{\phi}_{\mathrm{st}}^t \mathbf{M}^{\mathrm{FE}} \boldsymbol{\phi}_{\mathrm{st}} - 2\sum_{i=1}^{n-1} \frac{(\boldsymbol{\phi}_i^t \mathbf{M}^{\mathrm{FE}} \boldsymbol{\phi}_{\mathrm{st}})^2}{\boldsymbol{\phi}_i^t \mathbf{M}^{\mathrm{FE}} \boldsymbol{\phi}_i} + \sum_{i=1}^{n-1} \frac{(\boldsymbol{\phi}_i^t \mathbf{M}^{\mathrm{FE}} \boldsymbol{\phi}_{\mathrm{st}})^2}{\boldsymbol{\phi}_i^t \mathbf{M}^{\mathrm{FE}} \boldsymbol{\phi}_i} \\ &= \boldsymbol{\phi}_{\mathrm{st}}^t \mathbf{M}^{\mathrm{FE}} \boldsymbol{\phi}_{\mathrm{st}} - \sum_{i=1}^{n-1} \frac{(\boldsymbol{\phi}_i^t \mathbf{M}^{\mathrm{FE}} \boldsymbol{\phi}_{\mathrm{st}})^2}{\boldsymbol{\phi}_i^t \mathbf{M}^{\mathrm{FE}} \boldsymbol{\phi}_i} \\ &= \boldsymbol{\phi}_{\mathrm{st}}^t \mathbf{M}^{\mathrm{FE}} \boldsymbol{\phi}_{\mathrm{st}} - \sum_{i=1}^{n-1} m_i \end{aligned}$$

Appendix B. Stiffnesses $\{k_i\}_{i=0\ldots n-1}$

We consider the deformation energy $\mathscr{V}$ and the dof vector expansion (10):

$$\begin{aligned} \mathscr{V} &= \frac{1}{2}\boldsymbol{\psi}_0^t \mathbf{K}^{\mathrm{FE}} \boldsymbol{\psi}_0 \lambda_0^2 + \frac{1}{2}\sum_{i=1}^{N} (\lambda_i - \lambda_0)^2 \boldsymbol{\psi}_i^t \mathbf{K}^{\mathrm{FE}} \boldsymbol{\psi}_i + \sum_{i=1}^{N} (\lambda_i - \lambda_0)\lambda_0 \boldsymbol{\psi}_0^t \mathbf{K}^{\mathrm{FE}} \boldsymbol{\psi}_i \\ &= \frac{1}{2} k_0 \lambda_0^2 + \frac{1}{2}\sum_{i=1}^{N} (\lambda_i - \lambda_0)^2 k_i + \sum_{i=1}^{N} (\lambda_i - \lambda_0)\lambda_0 c_i \boldsymbol{\phi}_{\mathrm{st}}^t \mathbf{K}^{\mathrm{FE}} \boldsymbol{\phi}_i \end{aligned} \tag{B.1}$$

where the constraint mode orthogonality property is used. Moreover the static mode is orthogonal to the constraint vectors with respect to the stiffness matrix. Indeed,

$$\forall i \geqslant 1, \quad \boldsymbol{\phi}_{\mathrm{st}}^t \mathbf{K}^{\mathrm{FE}} \boldsymbol{\phi}_i = \boldsymbol{\phi}_i^t \mathbf{K}^{\mathrm{FE}} \boldsymbol{\phi}_{\mathrm{st}} = \boldsymbol{\phi}_i^t \mathbf{F}_{\mathrm{st}} = \boldsymbol{\phi}_{i\, i_0}^t \mathbf{F}_{\mathrm{st}\, i0} = 0 \tag{B.2}$$

where the definitions of $\mathbf{F}_{\mathrm{st}}$ and the constraint modes given by Eqs. (1) and (2) were used.

Then, the deformation energy is given by

$$\mathscr{V} = \frac{1}{2} k_0 \lambda_0^2 + \frac{1}{2}\sum_{i=1}^{n-1} (\lambda_i - \lambda_0)^2 k_i \tag{B.3}$$

Then the stiffnesses depicted in Fig. 1 can be defined as

- $$k_0 = \boldsymbol{\phi}_{\mathrm{st}}^t \mathbf{K}^{\mathrm{FE}} \boldsymbol{\phi}_{\mathrm{st}} \tag{B.4}$$

  - For statically determinate structures, k_0 is the static stiffness.
  - For statically indeterminate structures (i.e., $\boldsymbol{\phi}_{\mathrm{st}}$ is a rigid body eigenvector), $k_0 = 0$.

- $i = 1 \ldots n-1$:

$$k_i = \boldsymbol{\psi}_i^t \mathbf{K}^{\mathrm{FE}} \boldsymbol{\psi}_i = c_i^2 \boldsymbol{\phi}_i^t \mathbf{K}^{\mathrm{FE}} \boldsymbol{\phi}_i = c_i^2 \omega_{\mathrm{AR}\,i}^2 \boldsymbol{\phi}_i^t \mathbf{M}^{\mathrm{FE}} \boldsymbol{\phi}_i = \omega_{\mathrm{AR}\,i}^2 m_i \tag{B.5}$$

Moreover an eigenfrequency of a constraint mode is an antiresonance frequency [9]. Then the natural frequencies of the single-dof systems for $i = 1 \ldots n-1$ belong to the set of the antiresonant frequencies. This is why these systems are called "AOs".

Appendix C. Load vector $\mathbf{F}^{\mathrm{AO}}$

We consider the balance equation

$$\mathbf{M}^{\mathrm{FE}} \ddot{\mathbf{X}}(t) + \mathbf{K}^{\mathrm{FE}} \mathbf{X}(t) = \mathbf{F}(t) \tag{C.1}$$

Thus by multiplying Eq. (C.1) by $\boldsymbol{\phi}_i$ and using the expansion (9), the balance equation was

$$\sum_{j=0}^{n-1} \ddot{q}_j(t) \boldsymbol{\phi}_i^t \mathbf{M}^{\mathrm{FE}} \boldsymbol{\phi}_j + \sum_{j=0}^{n-1} q_j(t) \boldsymbol{\phi}_i^t \mathbf{K}^{\mathrm{FE}} \boldsymbol{\phi}_j = \boldsymbol{\phi}_i^t \mathbf{F}(t) \tag{C.2}$$

Then the definition of the different parameters can be used:

- $i = 0$:

$$m_0 \ddot{q}_0 + q_0 \left(k_{\mathrm{st}} - \sum_{j=1}^{n-1} k_j \right) - \sum_{j=1}^{n-1} q_j c_j \boldsymbol{\phi}_j^t \mathbf{K}^{\mathrm{FE}} \boldsymbol{\phi}_j = \boldsymbol{\phi}_0^t \mathbf{F} \tag{C.3}$$

So, in terms of λ_i:

$$m_0 \ddot{\lambda}_0 + k_{\mathrm{st}} \lambda_0 + \sum_{j=1}^{n-1} k_j (\lambda_0 - \lambda_j) = \boldsymbol{\phi}_0^t \mathbf{F} = \mathbf{F}_0^{\mathrm{AO}} \tag{C.4}$$

- $i > 0$:

$$\frac{m_i}{c_i^2} \ddot{q}_i + \frac{k_i}{c_i^2} q_i - \frac{k_i}{c_i^2} c_i q_0 = \boldsymbol{\phi}_i^t \mathbf{F} \tag{C.5}$$

The relation between q_i and λ_i leads to

$$m_i \ddot{\lambda}_i + k_i (q_i - q_0) = c_i \boldsymbol{\phi}_i^t \mathbf{F} = \mathbf{F}_i^{\mathrm{AO}} \tag{C.6}$$

Appendix D. A constraint mode defined by an eigenmode

Let $\{\boldsymbol{\phi}_j, \omega_j\}_{j=1\ldots n}$ be the eigenmodes of a structure normalised with respect to the mass matrix: $\boldsymbol{\phi}_i^t \mathbf{M}^{\mathrm{FE}} \boldsymbol{\phi}_i = 1$. We consider that $\{\boldsymbol{\phi}_i, \omega_i\}$ is the ith eigenmode, and that this is a constraint mode as well:

$$\boldsymbol{\phi}_{i\,i_0} = 0 \tag{D.1}$$

It has to be proved that

$$m_i = \frac{(\boldsymbol{\phi}_i^t \mathbf{M}^{\mathrm{FE}} \boldsymbol{\phi}_{\mathrm{st}})^2}{\boldsymbol{\phi}_i^t \mathbf{M}^{\mathrm{FE}} \boldsymbol{\phi}_i} = 0$$

i.e., that $\boldsymbol{\phi}_i$ and $\boldsymbol{\phi}_{\mathrm{st}}$ are orthogonal with respect to the mass matrix.

Some different cases have to be addressed:

(1) $\{\boldsymbol{\phi}_i, \omega_i\}$ is not a rigid body mode: $\omega_i \neq 0$.
$\boldsymbol{\phi}_{\mathrm{st}}$ may be expanded in terms of the eigenvectors:

$$\boldsymbol{\phi}_{\mathrm{st}} = \sum_{j=1}^{n} \alpha_j \boldsymbol{\phi}_j \tag{D.2}$$

We consider the product (D.3):

$$\boldsymbol{\phi}_i^t \mathbf{K}^{\mathrm{FE}} \boldsymbol{\phi}_{\mathrm{st}} = \alpha_i (\boldsymbol{\phi}_i^t \mathbf{K}^{\mathrm{FE}} \boldsymbol{\phi}_i) = \alpha_i \omega_i^2 \tag{D.3}$$

This product (D.3) is equal to zero. Indeed the static mode definition and relation (D.1) leads to

$$\boldsymbol{\phi}_i^t \mathbf{K}^{\mathrm{FE}} \boldsymbol{\phi}_{\mathrm{st}} = \boldsymbol{\phi}_i^t \mathbf{F}_{\mathrm{st}} = \boldsymbol{\phi}_{i\, i_0}^t \mathbf{F}_{\mathrm{st}\, i_0} = 0$$

Then α_i is equal to zero. So

$$m_i = \frac{(\boldsymbol{\phi}_i^t \mathbf{M}^{\mathrm{FE}} \boldsymbol{\phi}_{\mathrm{st}})^2}{\boldsymbol{\phi}_i^t \mathbf{M}^{\mathrm{FE}} \boldsymbol{\phi}_i} = (\alpha_i)^2 = 0$$

(2) $\{\boldsymbol{\phi}_i, \omega_i\}$ is a rigid body mode; hence $\{\boldsymbol{\phi}_i, \omega_i\}$ is an eigenmode as well. In that case $\boldsymbol{\phi}_{\mathrm{st}}$ is a rigid body mode of the structure as well. The eigenmode orthogonality properties lead immediately to the result:

$$m_i = 0$$

References

[1] T.J.R. Hughes, *The Finite Element Method*, Dover Publication, 2000.
[2] K.N. Shivakumar, W. Elber, W. Illg, Prediction of impact force and duration due to low-velocity impact on circular composites laminates, *Journal of Applied Mechanics* 52 (1985) 674–680.
[3] K.Q. Wu, T.X. Yu, Simple dynamic models of elastic plastic structures under impact, *International Journal of Impact Engineering* 25 (2001) 735–754.
[4] S. Abrate, Modeling of impacts on composite structures, *Composite Structures* 51 (2001) 129–138.
[5] S. Abrate, *Impact on Composite Structures*, Cambridge University Press, Cambridge, 1998.
[6] E. Jacquelin, J.P. Lainé, A. Bennani, M. Massenzio, A modelling of an impacted structure based on constraint modes, *Journal of Sound and Vibration* 301 (3–5) (2007) 789–802.
[7] E. Jacquelin, J.P. Lainé, A. Bennani, M. Massenzio, The anti-oscillator model parameters linked to the apparent mass frequency response function, *Journal of Sound and Vibration* 312 (4–5) (2008) 630–643.
[8] S. Pashah, M. Massenzio, E. Jacquelin, Structural response of impacted structure described through anti-oscillators, *International Journal of Impact Engineering* 35 (2008) 471–486.
[9] F. Wahl, G. Schmidt, L. Forrai, On the significance of antiresonance frequencies in experimental structural analysis, *Journal of Sound and Vibration* 219 (3) (1999) 379–394.